Journal of Drug Delivery Science and Technology 115 (2026) 107769

Contents lists available at ScienceDirect

Journal of Drug Delivery Science and Technology

journal homepage: www.elsevier.com/locate/jddst

Design and optimization of inherently cytotoxic nanostructured lipid carriers as drug vehicles with dual anti-cancer activity

John Youshia [a], Mera Medhat [b], Mariam George [b], Haidy Maged [b], Maureen Sherif [b], Salma Ashraf [b], Sara Ahmed [b], Marina George [b], Felopateer Karam [b], Wafaa Ibrahim [b], Mariam Samir [b], Dina O. Helal [a,c,*]

[a] Department of Pharmaceutics and Industrial Pharmacy, Faculty of Pharmacy, Ain Shams University, Cairo, Egypt
[b] Drug Design Program, Faculty of Pharmacy, Ain Shams University, Cairo, Egypt
[c] Leicester School of Pharmacy, Faculty of Health and life Sciences, De Montfort University, Leicestershire, United Kingdom

A R T I C L E I N F O

Keywords:
Breast cancer
Lipid nanocarriers
Curcumin
Lemon oil
Flaxseed oil
Blackseed oil

A B S T R A C T

Cancer remains to be one of the most life-threatening diseases with high rates of mortality and morbidity. The major challenge facing chemotherapy is targeting the drug molecules to malignant tissues and avoiding healthy ones. Optimal design of drug delivery carriers can assist not only in directing the drug moieties to the cancer cells but also in potentiating their action. In this study, we fabricated inherently cytotoxic nanostructured lipid carriers (NLCs) as nanovehicles for chemotherapeutic drugs for dual anticancer activity. Natural oils reported to have anticancer activity were used for the preparation of these cytotoxic nanovehicles, replacing conventionally used oils. Optimized NLCs impregnated with flaxseed or lemon oil had a size of 184 ± 10 and 167 ± 1 nm, respectively. Flaxseed oil impregnated NLCs lowered IC_{50} against MCF-7 breast cancer cells from 214 ± 65 μg oil/mL for conventional NLCs to 33 ± 12 μg oil/mL (6-fold enhancement), while lemon oil NLCs lowered it to 44 ± 17 μg oil/mL (5-fold enhancement). Loading both NLCs with curcumin, as a natural anticancer model drug, resulted in IC_{50} of 2.71 ± 1.8 and 2.79 ± 1.5 μg curcumin/mL for flaxseed and lemon oil, respectively This was lower than IC_{50} values recorded for free curcumin (12.93 ± 6.9 μg curcumin/mL) and curcumin loaded in conventional NLCs (7.21 ± 1.6 μg curcumin/mL). These results show that these designed cytotoxic nanovehicles can potentiate the chemotherapeutic action of any loaded drug, providing dual anticancer activity. They represent a promising drug delivery carrier in our fight against cancer.

1. Introduction

Cancer is the leading cause of death worldwide and is responsible for about 10 million deaths in 2020. The most common new cases are due to breast, lung, and colon cancer with breast cancer remaining one of the leading causes of cancer-related morbidity and mortality worldwide [1,2]. Early detection and treatment are critical to reduce mortality rates. Conventional cancer treatment strategies include surgery, radiation and chemotherapy [1]. However, the fundamental problem of chemotherapy is the lack of targeted delivery of the therapeutic agents selectively into the tumor tissue. This is essential to maintain effective drug concentration for a certain period and ensure drug-tumor interaction to perform anticancer activities with minimal systemic side effects. Luckily, tumors have a unique pathophysiological phenomenon called enhanced permeability and retention (EPR). This phenomenon makes the highly vascularized tumors permeable to macromolecular compounds, polymer conjugated drugs as well as nano-sized medications that can progressively accumulate within the tumor. Once inside the tumor, the reduced lymphatic drainage of the tumors keeps these compounds trapped inside the tumor tissue for a prolonged period of time [3]. This phenomenon can be taken advantage of to ensure efficient passive targeted delivery and retention of therapeutic agents to the tumors.

Lipid nanoparticles represent an opportunity as drug delivery carriers against cancer. They are biocompatible, easily manufactured and can be used for passive and active targeting of malignant tissues [4]. An interesting type is solid lipid nanoparticles (SLNs), which are composed of solid lipids stabilized by surfactant molecules on the surface.

* Corresponding author. Department of Pharmaceutics and Industrial Pharmacy, Faculty of Pharmacy, Ain Shams University, Cairo, Egypt.
E-mail address: dina.helal@dmu.ac.uk (D.O. Helal).

https://doi.org/10.1016/j.jddst.2025.107769
Received 7 April 2025; Received in revised form 28 October 2025; Accepted 9 November 2025
Available online 10 November 2025

However, owing to lipid recrystallization and formation of a perfect crystal lattice, drug expulsion may occur upon storage [5]. This was overcome by adding a liquid lipid or oil to the solid lipid to create imperfections in the crystal lattice and reduce the subsequent drug expulsion [6]. These nanoparticles represented the second generation of SLNs and were termed nanostructured lipid carriers (NLCs).

Natural-based compounds can target one or more of the mechanisms involved in cancer initiation and progression such as DNA damage, epigenetic modifications, metabolic alterations and chronic inflammation and thus suppress the initiation, progression, and even metastatic spread and relapse of cancers [1]. Several natural oils have shown antitumor activity against various human cancer cell lines [7,8]. Of particular interest are lemon, black seed, and flaxseed oils as they are edible and commonly consumed in various cuisines worldwide. In addition, their cytotoxicity against different cancer cell lines was previously reported. Lemon oil showed the highest cytotoxicity against human skin (A431), gastric (MKN-45) and brain (U-87 MG) cancer cell lines compared to other oils and was safe till a dose of 2000 mg/kg body weight [8]. Additionally, it was formulated in nanoemulsion and induced apoptosis in human lung cancer cells (A549) [9]. Black or *Nigella sativa* seed extracts were reported to have antitumor activity [10]. Moreover, its oil demonstrated cytotoxicity against human liver (HepG2) and breast (MCF-7) cancer cells with reported IC_{50} of 44.6 and 46.2 μg/mL, respectively and induced mitochondrial-mediated apoptosis in HepG2 cells [11]. Furthermore, chitosan [12] and gold [13] nanoparticles loaded with black seed oil recorded enhanced cytotoxicity and lower IC_{50} compared to free oil. Flaxseed oil inhibited proliferation of several cell lines of breast cancer, cervical cancer, and melanoma. Flow cytometry studies showed that flaxseed oil successfully induced apoptosis in murine melanoma (B16-BL6) and breast cancer cells (MCF-7) [14]. Moreover, it was safe on non-malignant cell lines and did not inhibit the growth of embryonic kidney cells (HEK293), human epithelial cells (HSG), and breast epithelial cells (HBL-100) [14]. Incorporating these oils into a suitable drug delivery system should facilitate their administration, protect them from enzymatic breakdown in physiological environment and target them to malignant tissues. It was previously reported that incorporating essential oil of *Pistacia atlantica* into NLCs significantly potentiated its anticancer activity. This was evident by declining the viability of SKBR3 breast cancer cells *via* cell cycle arrest and apoptosis, compared to cells treated with placebo and the free essential oil [15].

Our aim was to replace the commonly used oils in NLCs with natural oils having native anticancer activity namely lemon, black seed, and flaxseed oils to formulate NLCs with inherent cytotoxic activity, in other words cytotoxic nanovehicles. We hypothesize that this should augment the cytotoxic activity of NLCs and provide dual acting nanovehicles once loaded with an anticancer molecule. To the best of our knowledge, no one has attempted to prepare inherently cytotoxic NLCs and study the effect of combining these pharmacologically active nanovehicles with curcumin-a model natural cytotoxic drug- and study their combined cytotoxic effect. The effect of varying lipid concentration, type of oil and surfactant on the particle size and surface charge of NLCs was studied and analysed using design of experiments. Moreover, cytotoxicity of optimized formulae against human colon (Caco-2) and breast (MCF-7) cancer cell lines was evaluated. Furthermore, selected cytotoxic NLCs formulations were loaded with curcumin as a model natural drug with reported anticancer activity [16], to get a measure of the potential enhancement in cytotoxicity. This designed drug delivery system would offer dual anticancer activity against malignant tissues, where both the drug and the nanovehicles are cytotoxic to the cancer cells.

2. Materials and methods

2.1. Materials

Glyceryl behenate (Compritol® 888 ATO) and medium chain triglycerides (MCT) (Labrafac Lipophilie® WL 1349) were kindly gifted by Gattefosse (Saint-Priest Cedex, France). Curcumin was a kind gift from Eva Pharma (Cairo Egypt). Lemon oil, black seed oil and flaxseed oil were purchased from Imtenan (Cairo, Egypt). Poloxamer 188 (P188), sulforhodamine B and dimethylsulfoxide (DMSO) was purchased from Sigma-Aldrich (St. Louis, MO, USA). Penicillin/streptomycin were purchased from Capricorn scientific (Ebsdorfergrund, Germany). Fetal bovine serum (FBS) was purchased from Thermo Fisher scientific (Massachusetts, USA). Trypsin was purchased from Lonza (Verviers, Belgium). Roswell Park Memorial Institute (RPMI) and Dulbecco's Modified Eagle Medium (DMEM) were purchased from Serana (Pessin, Germany). Polysorbate 80 (P80), disodium hydrogen phosphate, potassium dihydrogen phosphate, sodium chloride and absolute ethanol were purchased from Adwic, El-Nasr Pharmaceutical Co. (Cairo, Egypt).

2.2. Preparation of NLCs

Hot high shear homogenization was the selected method for preparation of NLCs [17]. Briefly, lipid phase, composed of solid and liquid lipids, was heated to 80 °C on a hot plate (AREC.X VELP Scientifica, Usmate, Italy) to melt the solid lipid. The aqueous phase was heated to 85 °C and poured onto the lipid phase. Afterwards, the mixture was homogenized at 80 °C for 2 minutes at 10,000 rpm (Ultra Turrax T25, IKA, Germany). The obtained dispersion was then allowed to cool down at room temperature before being stored in the refrigerator at 4 °C for complete solidification and formation of NLCs. For curcumin-loaded formulations (Cur-NLCs), curcumin was added to the lipid phase during preparation.

2.2.1. Preliminary optimization of NLCs

Optimization of oil-impregnated NLCs was done in two steps. A preliminary experiment was performed using MCT, where the effect of two oil concentrations; 15 and 30 % of the lipid phase, was evaluated on the particle size of the prepared NLCs (MCT-NLCs). The lipid concentration (Glyceryl behenate + MCT) was fixed at 4 %, while the aqueous phase composition was fixed at 2 % P80.

2.2.2. Experimental design and construction of response surface one factor design

Based on preliminary optimization, the selected oil concentration (30 %) was used for further evaluation of other parameters. An experimental design using Design-Expert software version 13.0.5.0 (State-Ease Inc., Minneapolis, MN, USA) was employed to explore the response surfaces and the statistical models. The design included an independent numerical factor; (A) Lipid concentration (%) and two categorical factors; (B) Oil type and (C) Surfactant type. Factor A was tested at 3 numerical levels (low, intermediate, and high), factor B was tested using 3 different categorical levels namely; lemon oil, flaxseed oil and black seed oil whereas factor C was tested at only 2 levels as shown in Table 1. The oil concentration was fixed at 30 % of the total lipid phase. The evaluated responses were particle size and zeta potential.

L-NLCs, F-NLCs and B-NLCs are the respective assigned names in this manuscript for the NLCs prepared using lemon oil, flaxseed oil and black seed oil, respectively. A design matrix with a total of 30 different runs was generated by the software (Table S1). ANOVA was used for

Table 1
Levels of the formulation parameters for the preparation of NLCs using the response surface one factor design.

Factor	Type	Levels		
(A) Lipid concentration (%)	**Numeric**	3	4	5
(B) Surfactant type	**Categoric**	Polysorbate 80		Poloxamer 188
(C) Oil type	**Categoric**	Lemon	Flaxseed	Black seed

statistical authentication of the generated polynomial equations. The observed response was fitted to quadratic, linear and two-factor interactions (2FI) models. The interaction plots were constructed by the software and the polynomial equations were validated.

2.3. Physicochemical characterization of the prepared NLCs

NLCs were characterized for their particle size (PS), polydispersity index (PDI) using dynamic light scattering (DLS) technique as well as zeta potential (ξ) evaluation (Zetasizer Nano ZS, Malvern Instruments, Malvern, United Kingdom) [18]. To assess the physical stability of selected samples, measurements were carried out on freshly prepared samples and after storage at 4 °C for 1 and 3 months. Samples were diluted before measurement to avoid multiple scattering.

For determination of curcumin entrapment efficiency (EE, %) and drug loading (DL, %), NLCs were separated using centrifugal filters (Nanosep®, MWCO 100KD, Pall Life Sciences, New York, USA). Samples were centrifuged at 7000 rpm (4660 g) (Z216 MK, Hermle, Wehingen, Germany) at 20 °C for 60 minutes. The concentration of curcumin in the supernatant was measured in 50 % ethanol at a wavelength of 430 nm using spectrophotometry (UV-1601 PC, Shimadzu, Kyoto, Japan). This developed analytical method was validated in our laboratory and had a linearity range of 5–50 μg/mL. The limit of detection (LOD) and limit of quantification (LOQ) were found to be 3.25 μg/mL and 9.84 μg/mL, respectively. The regression equation ($R^2 = 0.997$) was:

$$y = 0.0137x + 0.0461$$

where, y is the absorbance and x is the concentration of curcumin in μg/mL.

EE and DL were calculated using the following equations [18]:

$$EE\ (\%) = \frac{W_t - W_f}{W_t} \times 100$$

$$DL\ (\%) = \frac{W_t - W_f}{W_n} \times 100$$

where: W_t is the total weight of curcumin used in the formulation, W_f is the weight of free curcumin remaining in the supernatant and W_n is the total weight of nanoparticles.

2.4. Transmission electron microscopy

Selected NLCs were examined under the electron microscope to study their morphology. Samples were bath-sonicated for 10 minutes (Crest Ultrasonics Corp., New Jersey, USA). Afterwards, a few drops were loaded on carbon coated copper grid, stained by 1 % phosphotungistic acid and left to dry. Then, the grid was examined by high resolution transmission electron microscope (HR-TEM) (JOEL, JEM-2100, Tokyo, Japan) operated at 200 KV [18].

2.5. In vitro release of curcumin from NLCs

Curcumin release from NLCs was performed through a dialysis membrane. A volume containing an equivalent of 0.25 mg curcumin, either free (Dissolved in the same composition of the dissolution medium) or loaded in NLCs was placed in a dialysis tube (MWCO 12,000–14,000, Spectra/Por®, Spectrum Laboratories, California, USA) and sunk in the dissolution medium. The dissolution medium was composed of 10 mL PBS containing 2 % P80. The pH was adjusted to 7.4 to mimic physiological blood conditions [19] and 6.5 to mimic tumor microenvironment [20]. While P80 was added to enhance solubility of curcumin and achieve sink conditions. The experiment setup was kept at 37 °C under continuous shaking at 100 strokes per minute (GFL 1083, Gesellschaft für Labortechnik, Burgwedel, Germany). Samples were withdrawn at the following time intervals (0.25, 0.5, 1, 2, 6, 24, 48, 72 and 120 hours at pH = 7.4/0.25, 0.5, 1, 2, 6, 24, 72, 96, 120, 168, 264 and 336 hours at pH = 6.5) and were replaced with fresh buffer to maintain sink conditions. The concentration of curcumin was assayed spectrophotometrically at 425 nm using a UV–Vis spectrophotometer. Two analytical methods were developed and validated in our laboratory for the assessment of curcumin at pH 7.4 and 6.5, respectively. At pH = 7.4, linearity range was 2.5–25 μg/mL. LOD and LOQ were found to be 1.71 μg/mL and 5.17 μg/mL, respectively. While at pH = 6.5, linearity range was 5–17.5 μg/mL. LOD and LOQ were found to be 1.55 μg/mL and 4.71 μg/mL, respectively. The regression equations were:

pH = 7.4	$y = 0.0457x - 0.0447$	$R^2 = 0.996$
pH = 6.5	$y = 0.0577x + 0.1226$	$R^2 = 0.992$

Where, y is the absorbance and x is the concentration of curcumin in μg/mL.

The mechanism of curcumin release was determined by fitting the data to different kinetic models using DDSolver Excel Add in [21]. Furthermore, the obtained release profiles were compared by calculating the difference factor (*f1*) and similarity factor (*f2*) according to the following equations [22].

$$f_1 = 100 \times \left\{ \left(\sum_{t=1}^{n} |R_t - T_t| \right) \Big/ \left(\sum_{t=1}^{n} R_t \right) \right\}$$

$$f_2 = 50 + \log\left\{ \left(1 + \frac{1}{n} \sum_{t=1}^{n} (R_t - T_t)^2 \right)^{-0.5} \times 100 \right\}$$

where n is the number of sampling time points, R_t and T_t are the mean percent curcumin released from reference (R) and test (T) products up to each time point t, respectively. To consider similar release profiles, *f1* values should fall between 0 and 15, while *f2* values should fall between 50 and 100.

2.6. Differential scanning calorimetry, fourier transform infrared spectroscopy and X-ray diffraction

Selected Cur-NLCs formulations, curcumin, glyceryl behenate, P188 and physical mixture (Composed of curcumin, glyceryl behenate and P188 in same percentage as NLCs formulations) were investigated using Fourier transform infrared spectroscopy (FTIR), differential scanning calorimetry (DSC), and X-ray diffraction (XRD). The aim was to study the crystallinity of NLCs and detect any incompatibility between the used ingredients [18]. Prior to characterization, curcumin-loaded NLCs were air dried under a flame hood into a solid powder.

Infrared spectrum of the samples was recorded after mixing with potassium bromide using FTIR spectrophotometer (Nicolet iS10, Thermo Fisher Scientific, Madison, WI, USA).

Thermal properties of the samples were investigated using differential scanning calorimetry (DSC-60 Plus; Shimadzu, Kyoto, Japan). Samples (3–5 mg) were sealed in aluminum pans with lids and heated at a rate of 10 °C/min to a temperature of 300 °C. The carrier gas was nitrogen with a flow rate of 30 mL/min.

Crystalline properties of the samples were measured using X-ray diffractometer (Empyrean 3, Malvern Panalytical B.V., Almelo, Netherlands). The scanning scope of 2θ for the diffraction pattern was between 5 and 90 at room temperature.

2.7. Cellular studies

2.7.1. Cell culture

Human colon (Caco-2) and breast (MCF-7) cancer cell lines were cultured in RPMI-1640, while human fibroblast normal cells (HFB4) were cultured in DMEM. Both media were supplemented with 100 μg/mL streptomycin, 100 units/mL penicillin and 10 % heat-inactivated fetal bovine serum and maintained in a 5 % (v/v) CO_2 humidified atmosphere at 37 °C.

2.7.2. Cell viability studies

Cytotoxicity of the selected oil-impregnated NLCs formulations and Cur-NLCs was tested on Caco-2 and MCF-7 cells using sulforhodamine B (SRB) assay [23]. Briefly, cells were seeded at a density of 2K cells/well in 96-well plates and left overnight. Subsequently, cells were treated with 0.1–1000 μg/mL of oil-impregnated NLCs or Cur-NLCs (equivalent to 0.005–50 μg Cur/mL) for 72 h. Eventually, cytotoxicity was assessed by adding SRB to the well plates, incubating for 48 h then the absorbance was measured at 545 nm using microplate reader (BioTek instruments, Vermont, USA). The results were expressed as the percentage cell survival and calculated using the following equation:

$$\text{Cell survival (\%)} = \frac{\text{Treated cells (A 545 nm)}}{\text{Untreated cells (A 545 nm)}} \times 100$$

Half-maximal inhibitory concentration (IC_{50}), the drug concentration at which 50 % growth inhibition is achieved, was calculated using GraphPad Prism software version 7.04 (GraphPad Software, La Jolla, California, USA).

Safety of the prepared Cur-NLCs was also assessed by evaluating their cytotoxicity on HFB4 cell line using the SRB assay as previously outlined.

2.8. Statistical analysis

Data are represented as mean ± standard deviation. Unpaired student t-test was used to analyze PS of NLCs stabilized by P80 and containing either 15 or 30 % MCT. In addition to analyzing cytotoxicity data of MCT-NLCs stabilized by P80 and P188 on MCF-7 and Caco-2 cells. While one-way ANOVA followed by Tukey's multiple comparisons test was utilized in analyzing the remaining cytotoxicity results. Analyses were done using GraphPad Prism version 7.04 (GraphPad Software, La Jolla, California, USA).

3. Results

3.1. Preliminary optimization of NLCs

MCT-NLCs prepared using 15 and 30 % oil of total lipid and stabilized by 2 % P80 showed PS of 249 ± 16 and 251 ± 1 nm, respectively. No significant difference ($p>0.05$) was found between both oil percentages. Accordingly, 30 % oil concentration was selected for further studies to maximize the loaded amount of the therapeutically active oil.

3.2. Effect of formulation parameters on particle size and zeta potential of NLCs

A full factorial experimental design was conducted using response surface one factor design to evaluate the effect and interactions of the different studied factors on PS and ξ of the prepared NLCs. The composition of the fabricated NLCs and their corresponding PS, PDI and ξ is shown in Table S1. The relation between the evaluated formulation parameters and the obtained size and charge was expressed using polynomial equations where; positive and negative coefficient signs indicate direct and inverse relationships between the evaluated responses and tested parameters, respectively [24] (Table S2). 2FI vs linear was the selected model for both responses ($p<0.05$) with a respective $R^2 = 0.91$ and 0.85 for PS and ξ, and an adequate precision of 15 and 10 for PS and ξ respectively, indicating a high signal to noise ratio thus, confirming its suitability to navigate the design space [25,26].

PS of the prepared NLCs ranged between 144 and 337 nm, while PDI ranged between 0.165 and 0.627. ANOVA of the PS data (Table S3) showed that both lipid concentration (A) and oil type (C) had a significant effect ($p<0.0001$) on PS, whereas the used surfactant type (B) had no significant effect ($p>0.05$). Moreover, interaction between the tested parameters was also evident where a significant interaction was found between A and C as well as between B and C ($p<0.05$). The 2D graphical illustrations, showing the relation between the three tested parameters and their interactions, are displayed in Fig. 1a and b.

PS increased significantly as lipid concentration increased from 3 to 5 % disregarding the type of surfactant used. For example: B-NLCs stabilized with 2 % P188 showed a successively increasing size of 193, 270 and 333 nm at respective 3, 4 and 5 % lipid concentration. Regarding the effect of oil type on PS, B-NLCs showed the largest PS, whereas L-NLCs were the smallest for both surfactants used. For instance, nanoparticles composed of 4 % lipid concentration and stabilized by P80 had PS of 216, 223 and 263 nm for L-NLCs, F-NLCs and B-NLCs respectively.

All the obtained particles were negatively charged with ξ values ranging between −14 and −38 mV. Both surfactant and oil types had a significant effect on ξ, whereas lipid concentration was found to have no significant effect as outlined in Table S4. NLCs prepared using P188 had significantly higher negative charge compared to their P80 counterparts for F-NLCs and B-NLCs (Fig. 1c and d). For instance, F-NLCs prepared using P188 had ξ of −32 vs −19 mV when prepared using P80 at 4 % lipid concentration. Oil type also had a significant effect, where the highest negative charge was obtained by flaxseed oil, followed by black seed oil and finally lemon oil. The relatively high zeta potential confers the stability of the prepared system.

The particles prepared using all the tested oils and surfactants were of suitable size for cellular uptake by cancer cells. However, increasing lipid concentration was found to increase PS beyond the desired limits. To select the most suitable and optimized formulae, we used the numerical optimization feature in Design Expert software. The desired criterion for selection was minimizing the PS. All proposed solutions suggested using 3 % lipid with various oil and surfactant types. Accordingly, 6 NLCs formulations composed of 3 % lipid concentration using lemon, black seed and flaxseed oil stabilized by either P80 or P188 were adopted in further studies to ensure proper cellular uptake.

3.3. Cytotoxicity of oil-impregnated NLCs

To avoid interference from surfactant type on the cytotoxicity results of the three oils, MCT-NLCs prepared using either P80 or P188 were assessed for their cytotoxic activity against Caco-2 and MCF-7 cell lines (Fig. S1). MCT-NLCs prepared with either surfactant showed non-significant ($p>0.05$) difference in cytotoxicity on MCF-7 cells. However, MCT-NLCs prepared using P80 were significantly more cytotoxic ($p<0.005$) on Caco-2 cell lines compared to P188 MCT-NLCs. Since P188 was found relatively safer on the tested cell lines, it was selected for further studies to exclude any cytotoxic effects imparted by the system to ensure proper evaluation of the cytotoxicity of the used cytotoxic agents either oils or curcumin.

Cytotoxicity and IC_{50} values of NLCs impregnated with the three cytotoxic oils were assessed against both cell lines and compared to MCT-NLCs (Fig. 2). Both F-NLCs and L-NLCs had respective IC_{50} of 33 ± 12 and 44 ± 17 μg oil/mL with significantly higher ($p<0.01$) cytotoxic activity against MCF-7 cells relative to the MCT-NLCs (IC_{50} = 214 ± 65 μg oil/mL). B-NLCs and MCT-NLCs showed similar cytotoxic activities on MCF-7 cell line. On the other side, F-NLCs (IC_{50} = 59 ± 14 μg oil/mL) were significantly more cytotoxic ($p<0.001$) on Caco-2 cells compared to MCT-NLCs, L-NLCs and B-NLCs with respective IC_{50} values of 275 ± 6, 259 ± 68 and 273 ± 19 μg oil/mL. Whereas, both L-NLCs and B-NLCs showed no significant difference ($p>0.05$) in cytotoxic activity on Caco-2 cells compared to the MCT-NLCs.

These findings indicate that both flaxseed and lemon oils were cytotoxic to MCF-7 cells while only flaxseed oil was cytotoxic to Caco-2 cells. Whereas black seed oil has no significant cytotoxicity on either tested cell lines. Accordingly, to augment the cytotoxic capabilities of F-NLCs and L-NLCs on MCF-7 cells, curcumin was incorporated in both F-

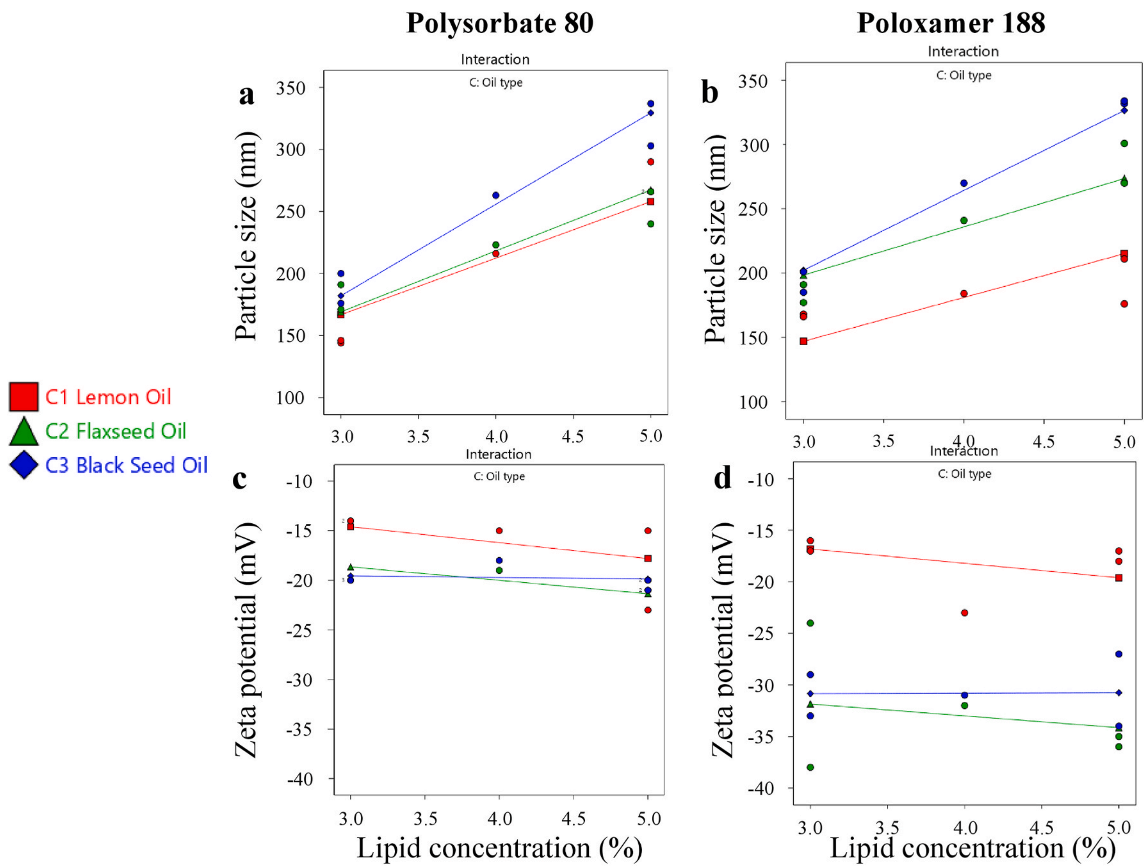

Fig. 1. 2D plot of the interaction of the different tested parameters on the particle size and zeta potential of the prepared oil-impregnated NLCs. NLCs were prepared using hot homogenization technique containing 30 % oil of total lipid content. Effect of oil type and lipid concentration on particle size of the prepared NLCs using (a) polysorbate 80 and (b) poloxamer 188. Effect of oil type and lipid concentration on zeta potential of the prepared NLCs using (c) polysorbate 80 and (d) poloxamer 188.

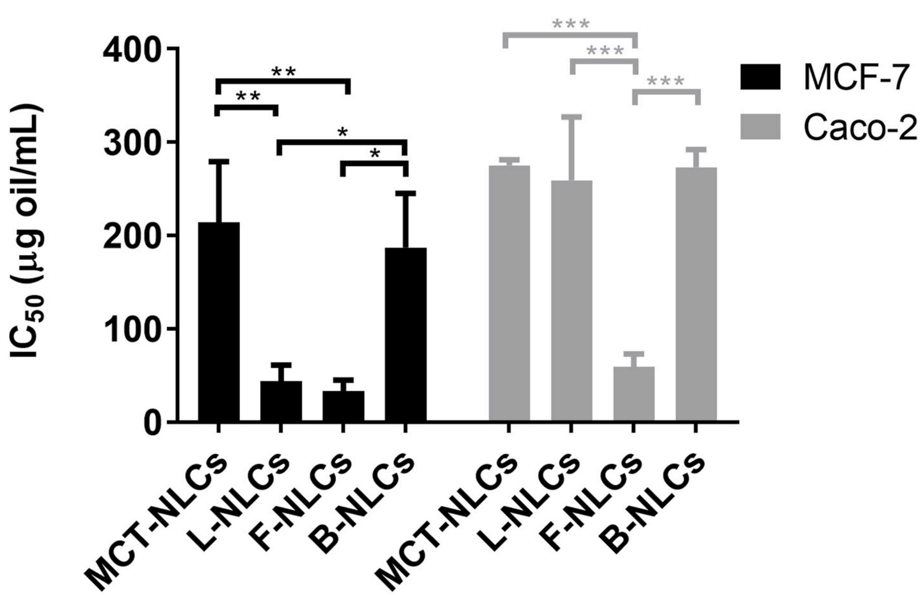

Fig. 2. Cytotoxicity of oil-impregnated NLCs tested by sulforhodamine B assay against MCF-7 and Caco-2 cells after incubation for 72 h. Results are presented as mean ± SD (n = 3) and were analysed using one-way ANOVA followed by Tukey's multiple comparisons.
MCT-NLCs: Medium chain triglycerides oil-NLCs L-NLCs: Lemon oil-NLCs
F-NLCs: Flaxseed oil-NLCs B-NLCs: Black seed oil-NLCs *$p < 0.05$, **$p < 0.01$, ***$p < 0.005$.

NLCs and L-NLCs.

3.4. Curcumin loaded NLCs

The composition of the curcumin loaded formulations along with their physicochemical properties are shown in Table 2. Increasing curcumin amount from 5 to 10 mg caused drug precipitation. Accordingly, 5 mg curcumin using both oil types was selected for further studies. Flaxseed oil impregnated particles loaded with curcumin (Cur-F-NLCs) showed a significantly higher ($p < 0.05$) PS of 269 ± 23 nm compared to 201 ± 28 nm obtained by lemon oil impregnated NLCs (Cur-L-NLCs). Measured PDI values were 0.358 and 0.415 for Cur-L-NLCs and Cur-F-NLCs, respectively with no significant difference between them. Zeta potential values of −32 ± 1 and −40 ± 1 mV were respectively obtained for Cur-L-NLCs and Cur-F-NLCs. Both formulations showed good physical stability showing non-significant changes in PS, PDI and ξ over 3 months storage at 4 °C (Fig. 3).

3.5. Transmission electron microscopy

Electron micrographs showed that F-NLCs and L-NLCs were spherical in shape with little to no aggregates. It is worth mentioning that the particle morphology did not change after curcumin loading (Fig. 4) and the PS obtained by TEM imaging was similar to that obtained by DLS.

3.6. In vitro release of curcumin from NLCs

At pH = 7.4, 100 % of curcumin was detected after 120 h in the release media of NLCs formulated from lemon oil and flaxseed oil versus 72 % from free curcumin (Fig. 5a). The release mechanism was best explained by Korsmeyer-Peppas model (Table 3). Based on the calculated 'n' values, the release of curcumin from its solution followed Fickian diffusion (n < 0.45), while curcumin release from both NLCs formulations followed non-Fickian diffusion (0.45<n < 0.89).

At pH 6.5, the release of curcumin was slower than that at pH 7.4. Where 43 %, 52 % and 56 % of curcumin was released after 336 h from free curcumin, Cur-L-NLCs and Cur F-NLCs, respectively (Fig. 5a). The release kinetics in case of free curcumin was best described by Korsmeyer-Peppas model following non-Fickian diffusion (0.45<n < 0.89). Release of curcumin from L-NLCs and F-NLCs could be fitted into two models, first-order and Korsmeyer-Peppas models for the former and Higuchi and Korsmeyer-Peppas models for the latter (Table 3).

By calculating the difference and similarity factors at either pH, it was found that the release profiles of curcumin from Cur-F-NLCs and Cur-L-NLCs were found to be similar to each other yet different from that of free curcumin (Table S5). Overall, loading curcumin in NLCs accelerated its release.

3.7. Fourier transform infrared spectroscopy

FTIR spectra were collected for glyceryl behenate, P188, curcumin, physical mixture and curcumin-loaded NLCs (Fig. 5b). Glyceryl behenate displayed a weak broad band around 3450 cm^{-1} indicating the presence of the hydroxy groups of mono/diglycerides of behenic acid. In addition to two strong bands at 2955 and 2850 cm^{-1}, characteristic of C-H symmetric and asymmetric stretching vibrations from the aliphatic chains of glyceryl behenate. Furthermore, a prominent band at approximately 1735 cm^{-1} corresponding to the C=O stretching of the ester links was obtained. P188 presented a weak broad O-H stretching vibration around 3400-3500 cm^{-1} attributable to its terminal hydroxyl groups. Distinct C-H stretching vibrations from both $-CH_2-$ and $-CH_3$ groups appear in the 2850-2950 cm^{-1} range. Moreover, a strong and broad C-O-C stretching band of ether bonds dominates the region between 1000 and 1200 cm^{-1}, characteristic of the polyether backbone. Curcumin exhibited its characteristic spectrum starting with a broad band around 3500 cm^{-1} indicating O-H stretching of its phenolic hydroxyl groups. A weak small band is evident at 2900 cm^{-1} owing to the C-H stretching. A sharp band at 1630 cm^{-1}, which corresponds to the C=O stretching of the conjugated diarylheptanoid structure, specifically the enolized β-diketone moiety, superimposed with C=C aromatic stretching. Both the physical mixture and NLCs showed superimposed band of their components. A broad O-H stretching vibration around 3300-3500 cm^{-1} owing to hydroxyl groups of glyceryl behenate and P188. Prominent strong C-H stretching bands between 2800 and 2950 cm^{-1} like that of glyceryl behenate and probably superimposing C-H stretching of P188. Both spectra showed a strong band at 1740 cm^{-1} representing C=O stretching of ester groups of glyceryl behenate. The stretching of C-O-C ether linkage was present around 1110 cm^{-1} in both spectra but was more prominent in the NLCs. It is worth mentioning that the characteristic peak of curcumin at 1630 cm^{-1} disappeared in both spectra.

3.8. Differential scanning calorimetry

DSC thermograms of glyceryl behenate, P188, curcumin, physical mixture and Cur-NLCs are presented in Fig. 5c. P188, glyceryl behenate, and curcumin showed sharp narrow endothermic troughs with high enthalpies at 62 °C (−1.16 J), 77 °C (−0.34 J) and 179 °C (−0.11 J) respectively, corresponding to their melting points and confirming their crystalline nature. Physical mixture showed two sharp narrow endothermic troughs at 58 °C (−0.26 J) and 76 °C (−0.23 J), corresponding to melting points of P188 and glyceryl behenate, respectively. It is worth mentioning that the endothermic trough of curcumin disappeared in the thermogram of physical mixture. Cur-NLCs showed small shallow endothermic troughs at 51 °C (−0.08 J) and 70 °C (−0.06 J) corresponding to P188 and glyceryl behenate respectively, with the disappearance of the curcumin endothermic trough.

3.9. X-ray diffraction

X-ray diffractograms of the samples analysed are provided in Fig. 5d. Glyceryl behenate showed two major sharp peaks. A more intense one at 2θ = 21° and lesser one at 2θ = 23° indicating its crystalline structure. Similarly, P188 showed two, almost equal, major peaks at 2θ = 19° and 23° with sharp intensities characteristic of a crystalline material. The diffractogram of curcumin was characterized by several sharp peaks indicating its crystalline nature. The two most prominent peaks were observed at 2θ = 9° and 17°. The physical mixture displayed 3 sharp

Table 2
Composition and physicochemical properties of curcumin loaded NLCs.

Formula code[a]	Cur (mg)	Oil (30 % of total lipid)	Entrapment efficiency (%) ± SD	Drug loading (%) ± SD	Particle size (nm) ± SD	Polydispersity index ± SD	Zeta potential (mV) ± SD
Cur-MCT-NLCs	5	Medium chain triglycerides	99 % ± 2	0.99 % ± 0.02	159 ± 5	0.233 ± 0.023	−27 ± 1
Cur-L-NLCs	5	Lemon oil	98 % ± 3	0.98 % ± 0.03	201 ± 28	0.358 ± 0.013	−32 ± 1
Cur-F-NLCs	5	Flaxseed oil	99 % ± 2	0.99 % ± 0.02	269 ± 23	0.415 ± 0.068	−40 ± 1
	10	Lemon oil	Drug precipitated				
	10	Flaxseed oil					

[a] NLCs were prepared using 3 % lipids and stabilized by 2 % poloxamer 188 as the surfactant.

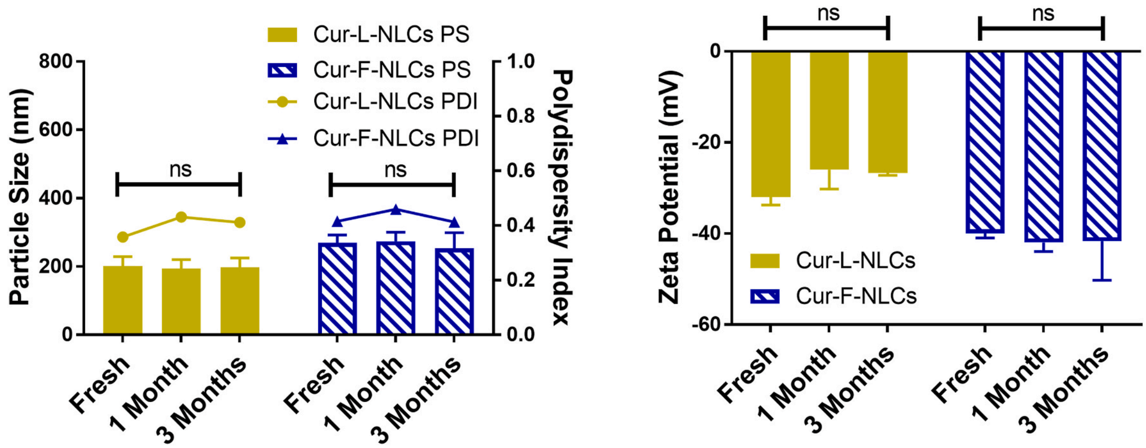

Fig. 3. Physical stability of curcumin loaded NLCs impregnated with lemon oil (Cur-L-NLCs) and flaxseed oil (Cur-F-NLCs). Measurement of particle size (PS), polydispersity index (PDI) and zeta potential were carried on fresh samples and after storage for 1 and 3 months at 4 °C. Results are expressed as mean ± SD (n = 3) and were analysed using 1-way ANOVA.
ns: not significant.

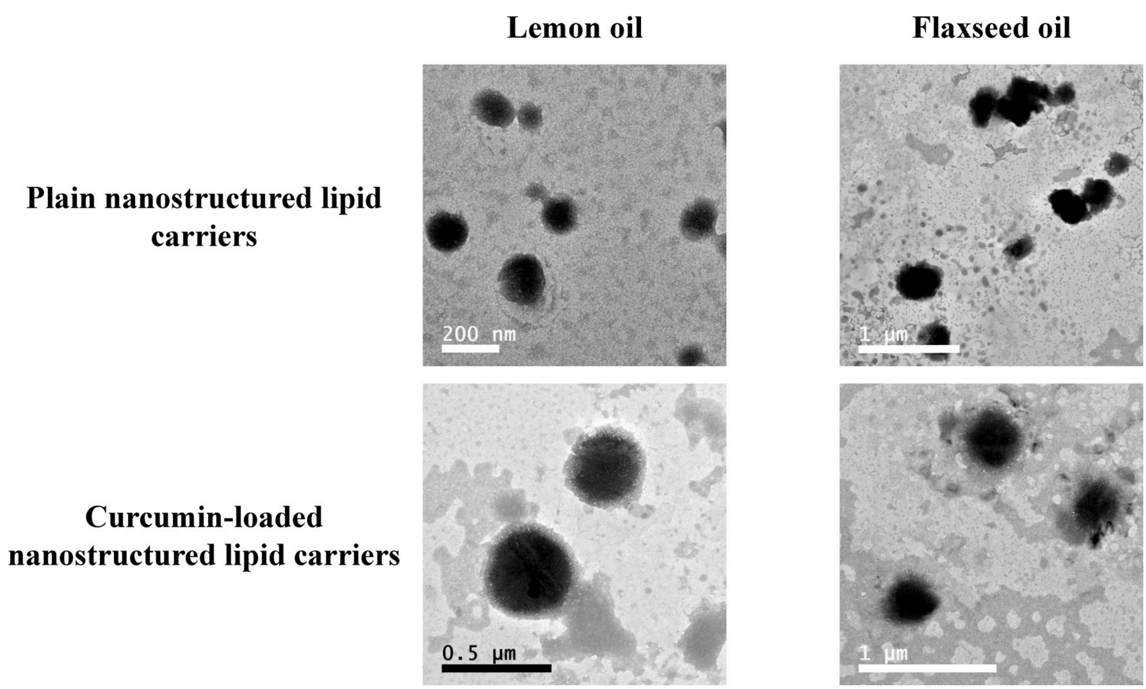

Fig. 4. Electron microscope images of plain and curcumin loaded NLCs.

intense peaks at 2θ = 19°, 21° and 23° conforming with the individual peaks of glyceryl behenate and P188. Overall, this indicates the preservation of the crystalline nature of the components of the physical mixture. Curcumin-loaded NLCs exhibited broadening of the peaks with a massive reduction of intensity at 2θ = 19° and 23° and disappearance of any peaks at 2θ = 21°. Similar to DSC, curcumin peaks were absent or diminished in the diffractograms of physical mixture and NLCs.

3.10. Cytotoxicity of curcumin-loaded NLCs

Cytotoxicity of Cur-F-NLCs and Cur-L-NLCs were compared to that of free curcumin as well as Cur-MCT-NLCs (Fig. 6 and Fig. S2). Incorporation of curcumin with either lemon oil or flaxseed oil in NLCs elevated the cytotoxic activity of the fabricated NLCs compared to free curcumin and Cur-MCT-NLCs. They lowered the IC_{50} values by 3 folds against Cur-MCT-NLCs and 5 folds against free curcumin. This is evident by the reduced IC_{50} values of 2.71 ± 1.84 and 2.79 ± 1.48 μg cur/mL for Cur-F-NLCs and Cur-L-NLCs, respectively against MCF-7 cells compared to the respective IC_{50} values of 12.93 ± 6.08 and 7.21 ± 1.4 μg cur/mL obtained by free curcumin and Cur-MCT-NLCs. Formulation of curcumin in NLCs impregnated with either lemon or flaxseed oil resulted in significantly higher cytotoxic activity ($p < 0.05$) against MCF-7 cells compared to free curcumin. On the other hand, curcumin formulated in conventional MCT-NLCs showed no significant difference in cytotoxic activity compared to free curcumin.

4. Discussion

In the past few decades, numerous colloidal systems such as liposomes, micro and nanoemulsions, polymeric nanoparticles, nanocapsules and nanosponges were investigated for use in cancer therapy. These systems have their own disadvantages such as; rapid degradation

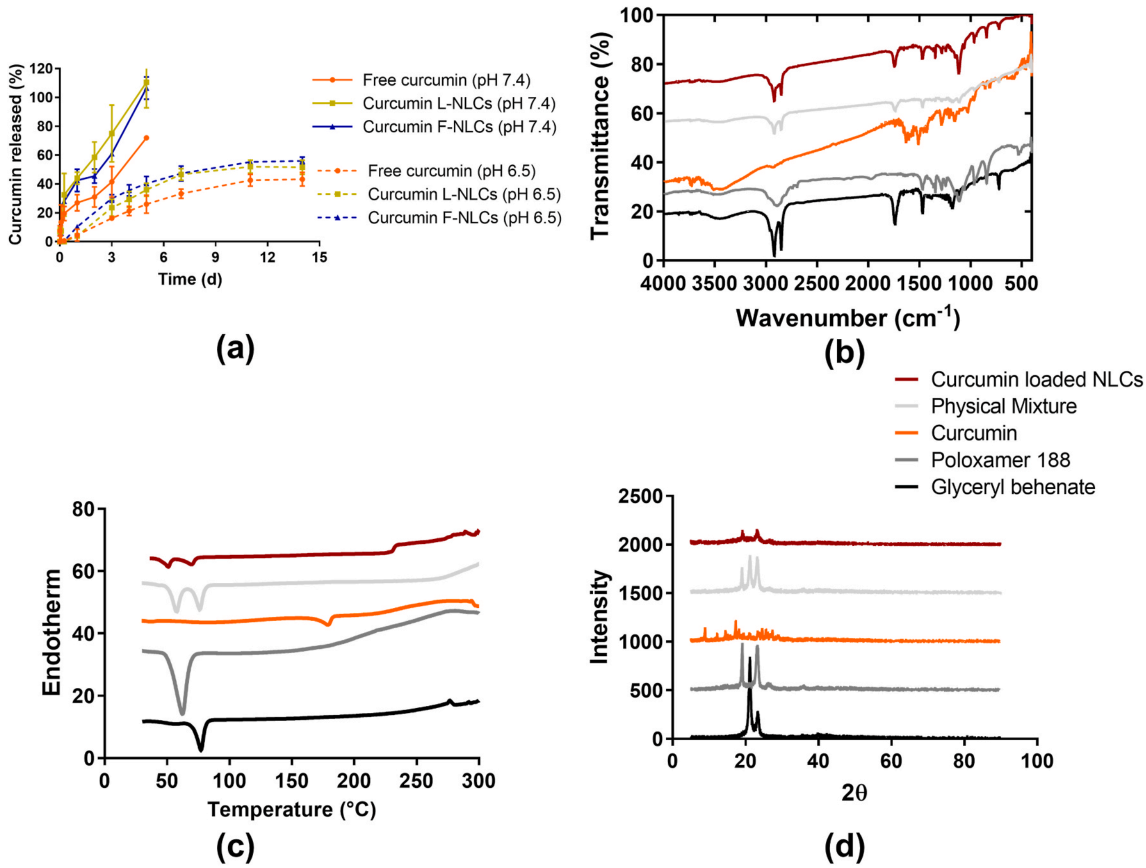

Fig. 5. **(a)** Cumulative release of curcumin either free or loaded in NLCs impregnated with lemon or flaxseed oils. **(b)** Fourier transform infrared spectroscopy, **(c)** Differential scanning calorimetry thermograms and **(d)** X-ray diffractograms of glyceryl behenate, poloxamer 188, curcumin, physical mixture (Curcumin, glyceryl behenate and poloxamer 188) and curcumin-loaded NLCs.

Table 3
R^2 values for fitted release data in different models.

pH	Formulation	Zero-order model	First-order model	Higuchi model	Korsmeyer-Peppas model
7.4	**Free curcumin**	0.68	0.74	0.92	0.95 n = 0.374
	Cur-L-NLCs	0.84	0.88	0.95	0.96 n = 0.529
	Cur-F-NLCs	0.90	0.88	0.93	0.94 n = 0.626
6.5	**Free curcumin**	0.92	0.97	0.95	0.98 n = 0.667
	Cur-L-NLCs	0.87	0.95	0.94	0.95 n = 0.604
	Cur-F-NLCs	0.84	0.94	0.97	0.97 n = 0.538

by the gastric pH or intestinal enzymes, limited large-scale production methods, fast drug release, stability difficulties as well as the residues of the organic solvents used in preparation [27]. All these points limit the use of these colloidal carriers in pharmaceutical drug delivery. Many of the aforementioned drawbacks are avoided in lipid nanoparticles, which have gained prominence in recent cancer research thanks to their small size and biocompatibility. NLCs offer multiple advantages over SLNs by introducing a liquid lipid/oil to the solid lipid matrix, thus creating a less organized matrix with increased number of imperfections in the crystal lattice, eventually, higher drug loading with reduced expulsion can be achieved [28].

Monotherapy approach is usually utilized for the treatment of various cancers. However, its non-selectively and poor specificity to the actively proliferating cells may result in the demolition of both healthy and cancerous cells. Accordingly, antitumor combination therapy-that combines two or more therapeutic agents-is recently proposed for effective cancer therapy. Besides its ability to deliver synergetic or additive effects, combination therapy could diminish the chances of drug resistance, reduce tumor growth and metastatic potential, reduce cancer stem cell populations and induce tumor cells apoptosis [29]. Accordingly, in this research project we aimed to replace the liquid lipid used in the inherent structure of NLCs with oils that have native cytotoxic activity to create cytotoxic nanovehicles. Moreover, these nanovehicles were further loaded with a model anticancer drug, curcumin, to further augment their therapeutic activity. In this case, dual cytotoxicity should arise from NLCs themselves and the loaded curcumin. Our target was to reach the highest oil/drug loading possible in the NLCs, while maintaining a PS around 200 nm to exploit EPR phenomenon and ensure their preferential uptake by cancer cells.

Curcumin was the model drug of choice due to its natural origin and possession of numerous antitumor properties. It can sensitize tumor cells to targeted therapy agents and reverse resistance to chemotherapeutic drugs [30]. Multiple studies reported that curcumin can be involved in inhibition of proliferation by regulating several signaling pathways, including PI3K/AKT, MAPK and nuclear factor (NF)-κB in addition to its ability to induce apoptosis [31,32]. Additionally, curcumin has synergistic effects with another chemotherapeutics. In breast cancer cell lines, curcumin and paclitaxel showed complementary effects on the alteration of proteins involved in apoptotic and inflammatory pathways [33]. Moreover, it was successfully incorporated in conventional NLCs and its cytotoxic activity against breast cancer was enhanced by photodynamic therapy [34].

Preliminary screening was performed to select the suitable oil percentage that can be incorporated in NLCs while maintaining a size <200 nm. Incorporating either 15 or 30 % oil yielded suitably sized NLCs with no significant difference in PS. This encouraged the selection of 30 % oil

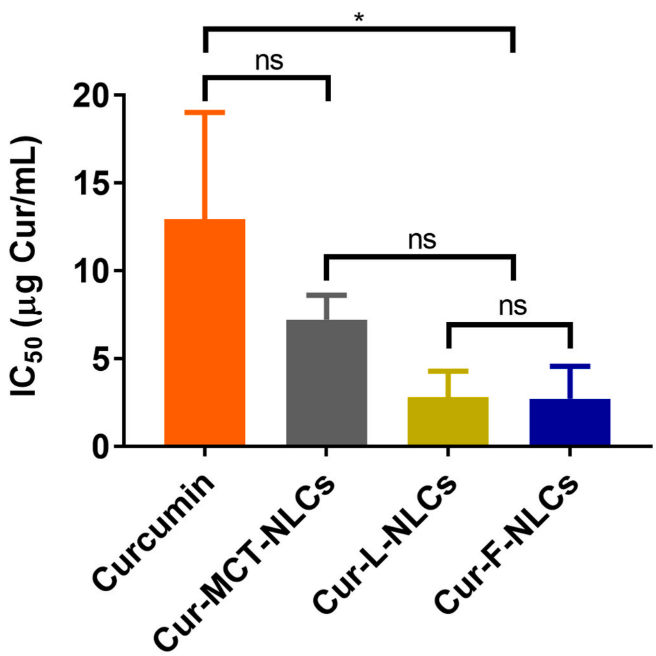

Fig. 6. Cytotoxicity of free curcumin (Cur) dissolved in dimethylsulfoxide and curcumin-loaded NLCs tested by sulforhodamine B assay against MCF-7 cells after incubation for 72 h. NLCs were diluted to provided Cur concentration equivalent 0.005–50 μg Cur/mL. Results are expressed as mean ± SD (n = 3) and were analysed using one-way ANOVA followed by Tukey's multiple comparisons.
MCT-NLCs: Medium chain triglycerides oil-NLCs L-NLCs: Lemon oil-NLCs
F-NLCs: Flaxseed oil-NLCs
ns: not significant, *$p < 0.05$.

to maximize loading of the native anticancer oils. In a previous study, it was also reported that increasing liquid lipid: solid lipid from 40:60 up to 60:40 did not have a significant effect on particle size of NLCs [35]. In another study, the use of different volumes of peppermint oil as the liquid lipid in NLCs was also reported to have no significant effect on the formulated NLCs. The addition of liquid lipids usually results in viscosity reduction which in turn reduce the dispersion energy needed to produce smaller particles. In our case it is assumed that the tested concentration of the liquid lipid did not have a major effect on the system viscosity and so no significant effect on PS was detected [36].

Glyceryl behenate was the solid lipid of choice owing to its biocompatibility, as it is generally regarded as safe and registered in the European and United States Pharmacopeias. Moreover, it is a versatile available excipient that has been already incorporated in several pharmaceutical and cosmetic formulations either available on the market or for research purposes [37]. Furthermore, it was previously selected for preparation of curcumin-loaded NLCs [38]. The range of 3–5 % lipid concentration was based on preliminary studies, where raising the lipid concentration above 5 % resulted in large NLCs with PS about 500 nm (Data not shown). Increasing lipid concentration from 3 to 5 % significantly increased PS. The size of NLCs is highly dependent on lipid concentration due to the increased tendency of the lipid to coalesce at high lipid concentration due to the difference in density between the internal and external phases according to Stoke's law [39]. The type of used oil also had a significant effect on NLCs' PS. This is mainly attributed to the nature of each oil, where the smallest size was obtained with lemon oil having viscosity 0.901cp [40] while that of black seed oil is 63.8 cp [41]. The difference in viscosity of the used oil affected the overall viscosity of the system thus the use of lemon oil resulted in the lowest viscosity and accordingly the smallest PS was obtained. On the other hand, the increased viscosity attained by the presence of black seed oil increased the PS of NLCs. Similarly, Akhoond et al. reported a difficulty in PS reduction during homogenization as the viscosity of the dispersed phase increased [42]. It is worth mentioning that similar behavior was also found with curcumin loaded NLCs where Cur-L-NLCs had smaller PS than their flaxseed counterparts. The insignificant effect of surfactant type on PS might be attributed to the similar non-ionic and hydrophilic nature of both used surfactants. Both P80 and P188 have ethylene oxide moieties in their structures that might have contributed to their identical distribution and behavior on the particles' surface resulting in insignificantly different PS [43,44]. Presence of ethylene oxide moiety might have resulted in an approximately similar contact angle value to the used lipids. It was previously reported that surfactants having similar contact angles could result in similarly sized NLCs [45]. Additionally, it was also reported that NLCs fabricated using a single surfactant -even with different nature-showed similar PS (160–180 nm), close to our reported PS range. However, upon mixing more than one surfactant type, they reported PS reduction and attributed this to the intercalation of non-ionic surfactant molecules between lipid chains [46]. PDI values indicate the size distribution of the samples. Values between 0.1 and 0.25 indicate narrow size distribution, while values over 0.5 indicates broad size distribution [47]. Overall, PDI values below 0.3 are favorable for nano-based formulations. [48]. There was a direct relationship between percentage of lipids and measured PDI. Generally, as lipid concentration was raised from 3 to 5 %, the PDI values increased from around 0.3 for 3 % lipid to around 0.5 for 5 % lipid.

Nanoparticles show good colloidal stability, when measured ξ values are ≥ +30 mV or ≤ −30 mV. This is particularly true for nanoparticles stabilized by ionic surfactants. While formulations stabilized by nonionic surfactants can still maintain good stability with ξ values outside of this optimal range owing to their steric stabilization. Where ξ > ±5 mV was reported to exhibit minimum flocculation tendency and high system stability [49]. This indicates the stability of our NLCs, which were stabilized by the nonionic surfactants P80 and P188. Changing the surfactant and oil types affected the obtained ξ. It was reported that incorporating high oil percentage in NLCs as 30 % in our NLCs might be associated with the formation of oil nano-compartments [50]. These nano-compartments can be present within the lipid matrix and/or on the surface affecting the ξ [50,51]. Both black seed and flaxseed oils are rich in fatty acids [52,53], while lemon oil is mainly composed of monoterpenes [54].The presence of these carboxylic groups in black seed and flaxseed oils might be the reason for the lower negative ξ values recorded for B-NLCs and F-NLCs compared to L-NLCs. Additionally, the discrepancy in the measured ξ values between P80 and P188 might be attributed to the tendency of P188 to form particles with a more negative surface charge [55].

Cytotoxic activity of lemon oil and flaxseed oil was previously reported on breast cancer cell lines [14,56]. This conforms to our results, where both L-NLCs and F-NLCs were cytotoxic to MCF-7 cells. The bioactive compounds present in lemon oil, such as limonene, citral, and terpineol, are strong anti-proliferative and apoptotic agents in cancer cells that might be accountable for its anticancer activity [56]. Whereas, treatment with flaxseed oil was reported to disrupt mitochondrial function in MCF-7 cells indicating that flaxseed oil can specifically inhibit cancer cell growth and induce apoptosis in some cancer cells [14]. Black seed oil, either pure or in nanoemulsion form, was previously reported to have cytotoxic activity on different cell lines including MCF-7 [10,57]. However, in our study B-NLCs were not cytotoxic to either MCF-7 or Caco-2 cells. Black seed oil is known for its cytotoxic behavior due to the presence of thymoquinone as its main constituent [58]. Other major constituents of black seed oil are linoleic acid and oleic acid representing 57.1 and 24.46 % of the oil respectively [53]. Linoleic acid was previously reported to act as a cell membrane fluidizer that could lower the energy cost of endocytosis and increase monocarboxylate transporter 1 expression on cell surfaces which in turn could increase the cellular uptake of the oil, contributing to its cytotoxic behavior [59]. Accordingly, the diminished cytotoxicity of B-NLCs on MCF-7 cells could be attributed to the masking of the membrane fluidizing properties of black seed oil within the NLCs which hindered its cellular uptake thus limiting the cytotoxic activity of the oil loaded NLCs. Assunção LS et al. have also reported similar behavior upon encapsulation of crude palm oil in nanoparticles. They proposed that cytotoxicity usually occurs due to the contact between fatty acids and cell membranes which in turn alters the lipid profile of the cell membrane, resulting in modified lipid-mediated signalling pathways, lipid peroxidation, and membrane fluidity, eventually reducing cellular viability [60]. Although the nanosized NLCs are supposed to have high cell penetration power, this phenomenon could be more potentiated *in vivo* by the EPR effect.

Curcumin-loaded NLCs displayed PS smaller than 300 nm, which is suitable for passive targeting of tumor tissue through the EPR effect. Although PDI values of Cur-L-NLCs and Cur-F-NLCs were larger than 0.3, they were still below 0.5 indicating moderate size distribution. According to FDA regulations, it is desirable for pharmaceutical nanocarriers to have PDI values below 0.3 suggesting the need for further optimization. Regarding curcumin's release from NLCs, it is known that reducing the particle size is associated with expansion of the total surface area. In addition, nanometric particles are characterized by their rapid movements due to Brownian motion. Both factors facilitated the dissolution and diffusion of curcumin, accelerating its release rate in comparison to its free solution at pH 7.4 and 6.5. It is known that curcumin undergoes keto-enol tautomerism, with the keto form more common in the acidic pH and enol form more common in the basic pH [61]. The keto form is characterized by lower aqueous solubility than the enol form, which might explain the slower release rate of curcumin at pH = 6.5 than at pH = 7.4 in accordance with previous reports [62]. Moreover, the Korsmeyer Peppas model was found to be the best fitting model for explaining the release mechanisms at pH = 7.4 based on the value of 'n', the release exponent. In case of free solution, curcumin release followed the Fickian diffusion depending on the concentration gradient. While curcumin release from NLCs followed non-Fickian diffusion. This indicates anomalous transport, where release is influenced by both diffusion of curcumin and erosion of the NLCs matrix. At pH = 6.5, the release of curcumin from NLCs was more complex and could be described by more than one model. Curcumin release from L-NLCs was described by both first order and Korsmeyer Peppas models, indicating dependency on amount of curcumin remaining and erosion of NLCs matrix. While curcumin release from F-NLCs was explained by both Higuchi and Korsmeyer Peppas models. Higuchi can be considered a specific case of Korsmeyer Peppas model when the value of 'n' approaches 0.5. This is indeed the case in Cur-F-NLCs (n = 0.538), which indicates that curcumin release followed Fickian diffusion from a matrix.

Analysis of functional groups using FTIR displayed characteristic spectra for glyceryl behenate, P188 and curcumin in accordance with previous reports. The characteristic bands of O-H, C-H and C=O stretching of glyceryl behenate and C-O-C stretching of P188 were preserved in the spectra of physical mixture and NLCs indicating the compatibility of the ingredients. The absence of the characteristic bands of curcumin in the FTIR of physical mixture and NLCs might be attributed to the small quantity of curcumin present relative to glyceryl behenate or P188. As the physical mixture was prepared using the same quantities of the curcumin-loaded NLCs. Melting points of glyceryl behenate, P188 and curcumin measured by DSC conform to previous reports [63–65]. Disappearance of curcumin trough in the physical mixture might be attributed to its dissolution in the melted glyceryl behenate. DSC thermogram of NLCs was characterized by small shallow troughs with small enthalpies. This ensured the reduction in crystallinity of glyceryl behenate and P188 and formation of defects in the crystal lattice owing to their incorporation in the NLCs [63,66]. Additionally, lowering of melting point compared to bulk samples is common and is attributed to the nano size range of NLCs [67]. Moreover, the vanishing of the curcumin melting trough indicates that it is either in an amorphous form or molecularly dispersed within the lipid matrix [63,66]. Obtained X-ray diffractograms for glyceryl behenate, P188 and curcumin indicated their crystalline nature and were similar to previous findings [65,68]. The physical mixture was also crystalline and displayed characteristic peaks of both glyceryl behenate and P188. The peak at $2\theta = 19^\circ$ is related to P188, while that at $2\theta = 21^\circ$ is related to glyceryl behenate. The peak at $2\theta = 23^\circ$ corresponds to both glyceryl behenate and P188. According to P188 individual diffractogram, its two peaks ($2\theta = 19^\circ$ and 23) are almost equivalent to each other in intensity, however in the physical mixture its peak at $2\theta = 23^\circ$ is more intense than the one at $2\theta = 19^\circ$. This is related to the contribution from the minor peak of glyceryl behenate present at the same angle. Curcumin-loaded NLCs diffractogram showed two peaks at $2\theta = 19^\circ$ and 23° attributed to P188 but their intensity was massively reduced in comparison to individual P188. Moreover, the main glyceryl behenate peak at $2\theta = 21^\circ$ was completely absent. This indicates a prominent reduction in the crystallinity of glyceryl behenate and P188 after incorporation in the NLCs conforming with DSC findings and previous reports [69]. The absence of curcumin peaks in the physical mixture and NLCs might be attributed to its presence in minor quantities in the physical mixture and incorporation in amorphous state within the matrix of the NLCs [65].

Dual loading of NLCs with both 1) cytotoxic natural oils namely lemon or flaxseed oil and 2) curcumin resulted in augmented anticancer activity of the nanocarriers against MCF-7 breast cancer cells. In a previous study, curcumin IC_{50} was reported to be 30.76 μg/ml, a value close to our findings [70]. Furthermore, conforming to our results, Mazzarino et al. reported no significant difference in cell viability after 72 h incubation of free curcumin and curcumin loaded lipid nanocapsules [71]. Curcumin was previously shown to have anticancer activities against numerous cell lines including breast cancer ones [70,72,73]. Moreover, it is known to have breast anticancer activities with different attributed mechanisms of action such as apoptosis induction, downregulation of intracellular transcription factors as well as disturbing the mitochondrial membrane [32]. Overall, these obtained results *in vitro* encourage further *in vivo* investigations in animal models at a dose of 5–10 mg/kg curcumin loaded into the NLCs [74,75].

The superior anticancer activity achieved by dual loading of curcumin in the oil-impregnated vehicles can be attributed to the enhanced cellular uptake of both agents in the nanosized lipidic carriers that favored curcumin delivery inside the cells. Moreover, the synergistic activity between curcumin and the used oils could have also resulted in the noticed superior activity. Similar findings were previously reported, where apigenin was loaded in NLCs formulated from rosehip oil, which is known for its antioxidant properties. The resulting formulation showed promising antiangiogenic and antiproliferative activities against cancer cells [76]. Additionally, NLCs containing thyme, sage and cinnamon essential oil were found to be effective against a xenograft model of prostate cancer [77]. These outcomes indicated a shift in the perception of the ingredients of NLCs, where they are no longer regarded as inactive excipients but as components that can potentiate the anticancer properties of the whole formulation. This necessitates further understanding of the molecular mechanisms behind the anticancer activity of the prepared system which is to be conducted in future studies.

5. Conclusion

In this work, we assessed the concept of preparing inherently cytotoxic NLCs using natural oils. Optimized nanoparticles impregnated with either lemon or flaxseed oil showed promising anticancer activity against MCF-7 breast cancer cells. Furthermore, they improved the cytotoxicity of the loaded curcumin over its free form. This proves the potential of these cytotoxic nanovehicles as drug carriers for dual cancer treatment. It should be noted that, due to the natural origin of the used oils and drug molecule, results might be variable by changing the origin of the used ingredients. Accordingly, further studies need to be conducted using different origins to confirm the obtained results. Moreover, future focus should include evaluating more oils and *in vivo* testing to further confirm the potential of clinical application of these nanocarriers.

CRediT authorship contribution statement

John Youshia: Writing – review & editing, Writing – original draft, Supervision, Methodology, Conceptualization. **Mera Medhat:** Data curation. **Mariam George:** Data curation. **Haidy Maged:** Data curation. **Maureen Sherif:** Data curation. **Salma Ashraf:** Data curation. **Sara Ahmed:** Data curation. **Marina George:** Data curation. **Felopateer Karam:** Data curation. **Wafaa Ibrahim:** Data curation. **Mariam Samir:** Data curation. **Dina O. Helal:** Writing – review & editing, Writing – original draft, Supervision, Methodology, Conceptualization.

Ethics approval

This is an *in vitro* study. No ethical approval is required.

Funding

This work was partially funded by the Drug Design Program, Faculty of Pharmacy, Ain Shams University.

Declaration of competing interest

The authors declare that they have no known competing financial interests or personal relationships that could have appeared to influence the work reported in this paper.

Appendix A. Supplementary data

Supplementary data to this article can be found online at https://doi.org/10.1016/j.jddst.2025.107769.

Data availability

The datasets generated during and/or analysed during the current study are available from the corresponding author on reasonable request.

References

[1] S.M. Samuel, P. Kubatka, D. Büsselberg, Treating cancers using nature's medicine: significance and challenges, Biomolecules 11 (2021) 1698, https://doi.org/10.3390/biom11111698.
[2] E.R. Timko Olson, A.A. Olson, M. Driscoll, A.L. Vermeesch, Nature-based interventions and exposure among cancer survivors: a scoping review, Int. J. Environ. Res. Publ. Health 20 (2023) 2376, https://doi.org/10.3390/ijerph20032376.
[3] J. Wu, The enhanced permeability and retention (EPR) effect: the significance of the concept and methods to enhance its application, J. Personalized Med. 11 (2021) 771, https://doi.org/10.3390/jpm11080771.
[4] S. Sheoran, S. Arora, R. Samsonraj, P. Govindaiah, S. Vuree, Lipid-based nanoparticles for treatment of cancer, Heliyon 8 (2022) e09403, https://doi.org/10.1016/j.heliyon.2022.e09403. England.
[5] K. Westesen, H. Bunjes, M.H.J. Koch, Physicochemical characterization of lipid nanoparticles and evaluation of their drug loading capacity and sustained release potential, J. Contr. Release 48 (1997) 223–236, https://doi.org/10.1016/S0168-3659(97)00046-1.
[6] V. Jenning, A.F. Thünemann, S.H. Gohla, Characterisation of a novel solid lipid nanoparticle carrier system based on binary mixtures of liquid and solid lipids, Int. J. Pharm. 199 (2000) 167–177, https://doi.org/10.1016/S0378-5173(00)00378-1.
[7] Y. Zu, H. Yu, L. Liang, Y. Fu, T. Efferth, X. Liu, et al., Activities of ten essential oils towards Propionibacterium acnes and PC-3, A-549 and MCF-7 cancer cells, Molecules 15 (2010) 3200–3210, https://doi.org/10.3390/molecules15053200.
[8] C. Manjunath, N. Mahurkar, In vitro cytotoxicity of cardamom oil, lemon oil, and jasmine oil on human skin, gastric, and brain cancer cell line, J. Cancer Res Ther 17 (2021). https://journals.lww.com/cancerjournal/Fulltext/2021/17010/In_vitro_cytotoxicity_of_cardamom_oil,_lemon_oil,.11.aspx.
[9] E. Yousefian Rad, M. Homayouni Tabrizi, P. Ardalan, S.M.R. Seyedi, S. Yadamani, P. Zamani-Esmati, et al., Citrus lemon essential oil nanoemulsion (CLEO-NE), a safe cell-depended apoptosis inducer in human A549 lung cancer cells with anti-angiogenic activity, J. Microencapsul. 37 (2020) 394–402, https://doi.org/10.1080/02652048.2020.1767223. Taylor & Francis.
[10] L. Ait Mbarek, H. Ait Mouse, N. Elabbadi, M. Bensalah, A. Gamouh, R. Aboufatima, et al., Anti-tumor properties of blackseed (Nigella sativa L.) extracts, Braz. J. Med. Biol. Res. Brazil 40 (2007) 839–847, https://doi.org/10.1590/s0100-879x2006005000108.
[11] M.M. Al-Oqail, E.S. Al-Sheddi, S.M. Al-Massarani, M.A. Siddiqui, J. Ahmad, J. Musarrat, et al., Nigella sativa seed oil suppresses cell proliferation and induces ROS dependent mitochondrial apoptosis through p53 pathway in hepatocellular carcinoma cells, South Afr. J. Bot. 112 (2017) 70–78, https://doi.org/10.1016/j.sajb.2017.05.019.
[12] A.M. Dawaba, H.M. Dawaba, Application of optimization technique to develop nano-based carrier of Nigella sativa essential oil: characterization and assessment. Recent pat drug deliv formul, United Arab Emirates 13 (2019) 228–240, https://doi.org/10.2174/1872211313666190516095309.
[13] S. Manju, B. Malaikozhundan, S. Vijayakumar, S. Shanthi, A. Jaishabanu, P. Ekambaram, et al., Antibacterial, antibiofilm and cytotoxic effects of Nigella sativa essential oil coated gold nanoparticles, Microb. Pathog. 91 (2016) 129–135, https://doi.org/10.1016/j.micpath.2015.11.021. England.
[14] A.L. Buckner, C.A. Buckner, S. Montaut, R.M. Lafrenie, Treatment with flaxseed oil induces apoptosis in cultured malignant cells, Heliyon 5 (2019) e02251, https://doi.org/10.1016/j.heliyon.2019.e02251.
[15] N. Najjari, S. Sari, M. Saffari, H. Kelidari, A. Nokhodchi, Formulation optimization and characterization of *Pistacia atlantica* desf. essential oil-loaded nanostructured lipid carriers on the proliferation of human breast cancer cell line SKBR3 (in vitro studies), J. Herb. Med. 36 (2022) 100600, https://doi.org/10.1016/j.hermed.2022.100600.
[16] T. Ming, Q. Tao, S. Tang, H. Zhao, H. Yang, M. Liu, et al., Curcumin: an epigenetic regulator and its application in cancer, Biomed. Pharmacother. 156 (2022) 113956, https://doi.org/10.1016/j.biopha.2022.113956.
[17] W. Mehnert, K. Mäder, Solid lipid nanoparticles: production, characterization and applications, Adv. Drug Deliv. Rev. 47 (2001) 165–196, https://doi.org/10.1016/S0169-409X(01)00105-3.
[18] M. Fawad, Z. Ali, F. Zahid, A.H. Alamri, A.A. Fatease, A.A. Lahiq, et al., Fabrication of oral sustained release capecitabine loaded nanostructured lipid carriers with improved bioavailability and prolonged anticancer effects, J. Mol. Liq. 421 (2025) 126852, https://doi.org/10.1016/j.molliq.2025.126852.
[19] T.H. Truong, K.P. Alcantara, B.P.I. Bulatao, F.N. Sorasitthiyanukarn, C. Muangnoi, N. Nalinratana, et al., Chitosan-coated nanostructured lipid carriers for transdermal delivery of tetrahydrocurcumin for breast cancer therapy, Carbohydr. Polym. 288 (2022) 119401, https://doi.org/10.1016/j.carbpol.2022.119401.
[20] Xie J, Li Y, Song L, Pan Z, Ye S, Hou Z. Design of a novel curcumin-soybean phosphatidylcholine complex-based targeted drug delivery systems. Drug Deliv. 24:707–719. https://doi.org/10.1080/10717544.2017.1303855.
[21] Y. Zhang, M. Huo, J. Zhou, A. Zou, W. Li, C. Yao, et al., DDSolver: an Add-In program for modeling and comparison of drug dissolution profiles, AAPS J. 12 (2010) 263–271, https://doi.org/10.1208/s12248-010-9185-1.
[22] J.W. Moore, H.H. Flanner, Mathematical comparison of dissolution profiles, Pharmaceut. Technol. 20 (1996) 64–74.
[23] V. Vichai, K. Kirtikara, Sulforhodamine B colorimetric assay for cytotoxicity screening, Nat. Protoc. 1 (2006) 1112–1116, https://doi.org/10.1038/nprot.2006.179.
[24] B. Sylvester, A. Porfire, M. Achim, L. Rus, I. Tomuţă, A step forward towards the development of stable freeze-dried liposomes: a quality by design approach (QbD), Drug Dev. Ind. Pharm. 44 (2018) 385–397, https://doi.org/10.1080/03639045.2017.1395457.
[25] A. Rai, B. Mohanty, R. Bhargava, Modeling and response surface analysis of supercritical extraction of watermelon seed oil using carbon dioxide, Separ. Purif. Technol. 141 (2015) 354–365, https://doi.org/10.1016/j.seppur.2014.12.016.
[26] D. Leng, K. Thanki, E. Fattal, C. Foged, M. Yang, Engineering of budesonide-loaded lipid-polymer hybrid nanoparticles using a quality-by-design approach, Int. J. Pharm. 548 (2018) 740–746, https://doi.org/10.1016/j.ijpharm.2017.08.094.
[27] S. Selvamuthukumar, R. Velmurugan, Nanostructured lipid carriers: a potential drug carrier for cancer chemotherapy, Lipids Health Dis. 11 (2012) 159, https://doi.org/10.1186/1476-511X-11-159.
[28] S. Lucks, R. Muller, Medication vehicles made of solid lipid particles (solid lipid nanospheres - SLN) [internet]. https://patents.google.com/patent/AU672177B2/en/enIt.pdf, 1996. (Accessed 24 February 2024).
[29] M. Li, G. Fang, F. Zahid, R. Saleem, G. Ishrat, Z. Ali, et al., Co-delivery of paclitaxel and curcumin loaded solid lipid nanoparticles for improved targeting of lung cancer: in vitro and in vivo investigation, Heliyon 10 (2024) e30290, https://doi.org/10.1016/j.heliyon.2024.e30290. Elsevier [cited 2025 July 7].
[30] Q.-M. Zhou, X.-F. Wang, X.-J. Liu, H. Zhang, Y.-Y. Lu, S. Huang, et al., Curcumin improves MMC-Based chemotherapy by simultaneously sensitising cancer cells to MMC and reducing MMC-Associated side-effects, Eur. J. Cancer 47 (2011) 2240–2247, https://doi.org/10.1016/j.ejca.2011.04.032. Elsevier.
[31] G.P. Nagaraju, S. Aliya, S.F. Zafar, R. Basha, R. Diaz, B.F. El-Rayes, The impact of curcumin on breast cancer, Integr Biol (Camb). 4 (2012) 996–1007, https://doi.org/10.1039/c2ib20088k.
[32] A.B. Kunnumakkara, D. Bordoloi, G. Padmavathi, J. Monisha, N.K. Roy, S. Prasad, et al., Curcumin, the golden nutraceutical: multitargeting for multiple chronic diseases, Br. J. Pharmacol. 174 (2017) 1325–1348, https://doi.org/10.1111/bph.13621.
[33] E.T. Quispe-Soto, G.M. Calaf, Effect of curcumin and paclitaxel on breast carcinogenesis, Int. J. Oncol. 49 (2016) 2569–2577, https://doi.org/10.3892/ijo.2016.3741.

[34] A.E. Kamel, M. Fadel, D. Louis, Curcumin-loaded nanostructured lipid carriers prepared using Peceol™ and olive oil in photodynamic therapy: development and application in breast cancer cell line, Int. J. Nanomed. 14 (2019) 5073–5085, https://doi.org/10.2147/IJN.S210484. Dove Medical Press.
[35] D.P.C. de Barros, P. Reed, M. Alves, R. Santos, A. Oliva, Biocompatibility and antimicrobial activity of nanostructured lipid carriers for topical applications are affected by type of oils used in their composition, Pharmaceutics 13 (2021) 1950, https://doi.org/10.3390/pharmaceutics13111950.
[36] T. Erawati, R.A. Arifiani, A. Miatmoko, D.M. Hariyadi, N. Rosita, T. Purwanti, The effect of peppermint oil addition on the physical stability, irritability, and penetration of nanostructured lipid carrier coenzyme Q10, J. Publ. Health Afr. 14 (2023) 8, https://doi.org/10.4081/jphia.2023.2515.
[37] Compritol 888 ATO: a multifunctional lipid excipient in drug delivery systems and nanopharmaceuticals: Expet Opin. Drug Deliv.: Vol 11, No 12 [Internet]. [cited 2025 July 9]. https://www.tandfonline.com/doi/10.1517/17425247.2014.935335?url_ver=Z39.88-2003&rfr_id=ori:rid:crossref.org&rfr_dat=cr_pub%20%200pubmed. Accessed 9 July 2025.
[38] P. Lakhani, A. Patil, P. Taskar, E. Ashour, S. Majumdar, Curcumin-loaded nanostructured lipid carriers for ocular drug delivery: design optimization and characterization, J. Drug Deliv. Sci. Technol. 47 (2018) 159–166, https://doi.org/10.1016/j.jddst.2018.07.010.
[39] J. Emami, H. Mohiti, H. Hamishehkar, J. Varshosaz, Formulation and optimization of solid lipid nanoparticle formulation for pulmonary delivery of budesonide using taguchi and box-behnken design, Res. Pharm. Sci. 10 (2015) 17–33.
[40] A.A. Permanasari, S. Sukarni, R. Wulandari, P. Puspitasari, M.N. Mauludi, R. Ramadani, Density, flash point, viscosity, and heating value of waste cooking biodiesel (B20) with bioadditive essential oil (lemon, lemongrass, eucalyptus), J. Phys.: Conf Ser. 1595 (2020) 012005, https://doi.org/10.1088/1742-6596/1595/1/012005.
[41] W. Zzaman, T. Yang, Physicochemical and quality characteristic s of cold and hot press of Nigella sativa L seed oil using screw press, J. Appl. Sci. Res. 10 (2014).
[42] Zardini A. Akhoond, M. Mohebbi, R. Farhoosh, S. Bolurian, Production and characterization of nanostructured lipid carriers and solid lipid nanoparticles containing lycopene for food fortification, J. Food Sci. Technol. 55 (2018) 287–298, https://doi.org/10.1007/s13197-017-2937-5.
[43] T.K. Lind, E.J. Nilsson, B. Wyler, D. Scherer, T. Skansberger, M. Morin, et al., Effects of ethylene oxide chain length on crystallization of polysorbate 80 and its related compounds, J. Colloid Interface Sci. 592 (2021) 468–484, https://doi.org/10.1016/j.jcis.2021.01.065.
[44] B. Erlandsson, Stability-indicating changes in poloxamers: the degradation of ethylene oxide-propylene oxide block copolymers at 25 and 40 °C, Polym. Degrad. Stabil. 78 (2002) 571–575, https://doi.org/10.1016/S0141-3910(02)00233-1.
[45] P. Riangjanapatee, S. Okonogi, Effect of surfactant on lycopene-loaded nanostructured lipid carriers, Drug Discov. Ther. 6 (2012) 163–168.
[46] K. Karn-orachai, S.M. Smith, S. Phunpee, A. Treethong, S. Puttipipatkhachorn, S. Pratontep, et al., The effect of surfactant composition on the chemical and structural properties of nanostructured lipid carriers, J. Microencapsul. 31 (2014) 609–618, https://doi.org/10.3109/02652048.2014.911374. Taylor & Francis.
[47] B. Hoseini, M.R. Jaafari, A. Golabpour, A.A. Momtazi-Borojeni, M. Karimi, S. Eslami, Application of ensemble machine learning approach to assess the factors affecting size and polydispersity index of liposomal nanoparticles, Sci. Rep. 13 (2023) 18012, https://doi.org/10.1038/s41598-023-43689-4. Nature Publishing Group.
[48] N. Raval, R. Maheshwari, D. Kalyane, S.R. Youngren-Ortiz, M.B. Chougule, R. K. Tekade, Chapter 10 - importance of physicochemical characterization of nanoparticles in pharmaceutical product development, in: R.K. Tekade (Ed.), Basic Fundamentals of Drug Delivery [Internet], Academic Press, 2019, pp. 369–400, https://doi.org/10.1016/B978-0-12-817909-3.00010-8 [cited 2025 July 9].
[49] R.H. Müller, K. Mäder, S. Gohla, Solid lipid nanoparticles (SLN) for controlled drug delivery – a review of the state of the art, Eur. J. Pharm. Biopharm. 50 (2000) 161–177, https://doi.org/10.1016/S0939-6411(00)00087-4.
[50] R.H. Müller, M. Radtke, S.A. Wissing, Solid lipid nanoparticles (SLN) and nanostructured lipid carriers (NLC) in cosmetic and dermatological preparations, Adv. Drug Deliv. Rev. 54 (2002) S131–S155, https://doi.org/10.1016/S0169-409X(02)00118-7.
[51] K. Jores, W. Mehnert, M. Drechsler, H. Bunjes, C. Johann, K. Mäder, Investigations on the structure of solid lipid nanoparticles (SLN) and oil-loaded solid lipid nanoparticles by photon correlation spectroscopy, field-flow fractionation and transmission electron microscopy, J. Contr. Release 95 (2004) 217–227, https://doi.org/10.1016/j.jconrel.2003.11.012.
[52] S. Al-Madhagy, N.S. Ashmawy, A. Mamdouh, O.A. Eldahshan, M.A. Farag, A comprehensive review of the health benefits of flaxseed oil in relation to its chemical composition and comparison with other omega-3-rich oils, Eur. J. Med. Res. 28 (2023) 240, https://doi.org/10.1186/s40001-023-01203-6.
[53] Z. Albakry, E. Karrar, I.A.M. Ahmed, E. Oz, C. Proestos, A.F. El Sheikha, et al., Nutritional composition and volatile compounds of black cumin (Nigella sativa L.) seed, fatty acid composition and tocopherols, polyphenols, and antioxidant activity of its essential oil, Horticulturae 8 (2022) 575, https://doi.org/10.3390/horticulturae8070575. Multidisciplinary Digital Publishing Institute.
[54] A. Ben Hsouna, N. Ben Halima, S. Smaoui, N. Hamdi, Citrus lemon essential oil: chemical composition, antioxidant and antimicrobial activities with its preservative effect against Listeria monocytogenes inoculated in minced beef meat, Lipids Health Dis. 16 (2017) 146, https://doi.org/10.1186/s12944-017-0487-5.
[55] Production and optimization of valproic acid nanostructured lipid carriers by the taguchi design: Pharmaceutical development and technology: Vol 15 , No 1 - Get Access [Internet]. [cited 2025 July 9]. https://www.tandfonline.com/doi/full/10.3109/10837450903013568. Accessed 9 July 2025.
[56] A. Narayanankutty, N.U. Visakh, A. Sasidharan, B. Pathrose, O.J. Olatunji, A. Al-Ansari, et al., Chemical composition, antioxidant, anti-bacterial, and anti-cancer activities of essential oils extracted from citrus limetta risso peel waste remains after commercial use, Molecules (2022), https://doi.org/10.3390/molecules27238329, 27:8329.
[57] V.S. Periasamy, J. Athinarayanan, A.A. Alshatwi, Anticancer activity of an ultrasonic nanoemulsion formulation of Nigella sativa L. essential oil on human breast cancer cells, Ultrason. Sonochem. 31 (2016) 449–455, https://doi.org/10.1016/j.ultsonch.2016.01.035.
[58] M. Esmaeli, A. Ghanbari, M. Barazesh, M.D. Dehabadi, Nigella sativa (black seed) and breast cancer: a systematic review, Indian J. Gynecol Oncolog 22 (2024) 154, https://doi.org/10.1007/s40944-024-00920-y.
[59] H. Yuan, P. Xiao, F. Wang, C. Guo, S. Pan, M. Jiang, et al., Linoleic acid co-administration promotes oral delivery of exenatide-loaded butyrate-decorated nanocapsules, J. Contr. Release 382 (2025) 113744, https://doi.org/10.1016/j.jconrel.2025.113744.
[60] L.S. Assunção, C.D.F. Ribeiro, C.O. de Souza, R. Danielski, S. Kumari, I.L. Nunes, et al., Nanoencapsulation of hybrid crude palm oil unaué HIE OxG with jackfruit by-products as encapsulants: a study of cellular antioxidant activity and cytotoxicity in Caco-2 cells, Food Chem. 448 (2024) 139009, https://doi.org/10.1016/j.foodchem.2024.139009.
[61] M.D. Ciuca, R.C. Racovita, Curcumin: overview of extraction methods, health benefits, and encapsulation and delivery using microemulsions and nanoemulsions, Int. J. Mol. Sci. 24 (2023) 8874, https://doi.org/10.3390/ijms24108874.
[62] T.T.T. Mai, K.S. Phan, B.T. Doan, T.T.H. Le, T.D.T. Ung, Q.B.N. Nguyen, et al., Multifunctional quantum dot-decorated drug-loaded magnetite nanosystem for dual optical-magnetic resonance imaging and drug delivery, RSC Adv. The Royal Soc. Chem. 15 (2025) 21269–21283, https://doi.org/10.1039/D5RA03379A.
[63] J. Youshia, A.O. Kamel, A. El Shamy, S. Mansour, Gamma sterilization and in vivo evaluation of cationic nanostructured lipid carriers as potential ocular delivery systems for antiglaucoma drugs, Eur. J. Pharmaceut. Sci. 163 (2021) 105887, https://doi.org/10.1016/j.ejps.2021.105887.
[64] U. Ilyas, M. Asif, M. Wang, R. Altaf, H. Zafar, M.M. Faran Ashraf Baig, et al., Nanostructured lipid carrier-based delivery of pioglitazone for treatment of type 2 diabetes, Front. Pharmacol. 13 (2022) 934156, https://doi.org/10.3389/fphar.2022.934156. Switzerland.
[65] M. Agrawal, S. Saraf, M. Pradhan, R.J. Patel, G. Singhvi, Ajazuddin, et al., Design and optimization of curcumin loaded nano lipid carrier system using box-behnken design, Biomed. Pharmacother. 141 (2021) 111919, https://doi.org/10.1016/j.biopha.2021.111919.
[66] J. Youshia, A.O. Kamel, A. El Shamy, S. Mansour, Design of cationic nanostructured heterolipid matrices for ocular delivery of methazolamide, Int. J. Nanomed. 7 (2012) 2483–2496, https://doi.org/10.2147/IJN.S28307.
[67] H. Bunjes, T. Unruh, Characterization of lipid nanoparticles by differential scanning calorimetry, X-ray and neutron scattering, Adv. Drug Deliv. Rev. 59 (2007) 379–402, https://doi.org/10.1016/j.addr.2007.04.013.
[68] U. Ilyas, M. Asif, M. Wang, R. Altaf, H. Zafar, Ashraf Baig MM. Faran, et al., Nanostructured lipid carrier-based delivery of pioglitazone for treatment of type 2 diabetes, Front Pharmacol. Frontiers 13 (2022), https://doi.org/10.3389/fphar.2022.934156 [cited 2025 July 9].
[69] S. Rubab, K. Naeem, I. Rana, N. Khan, M. Afridi, I. Ullah, et al., Enhanced neuroprotective and antidepressant activity of curcumin-loaded nanostructured lipid carriers in lipopolysaccharide-induced depression and anxiety rat model, Int. J. Pharm. 603 (2021) 120670, https://doi.org/10.1016/j.ijpharm.2021.120670.
[70] Koohpar Z. Khazaei, M. Entezari, A. Movafagh, M. Hashemi, Anticancer activity of curcumin on human breast adenocarcinoma: role of Mcl-1 gene, Iran. J. Cancer Prev. 8 (2015) e2331, https://doi.org/10.17795/ijcp2331.
[71] L. Mazzarino, L.F.C. Silva, J.C. Curta, M.A. Licínio, A. Costa, L.K. Pacheco, et al., Curcumin-loaded lipid and polymeric nanocapsules stabilized by nonionic surfactants: an *in vitro* and *in vivo* antitumor activity on B16-F10 melanoma and macrophage uptake comparative study, J. Biomed. Nanotechnol. 7 (2011) 406–414, https://doi.org/10.1166/jbn.2011.1296.
[72] S. Hu, Y. Xu, L. Meng, L. Huang, H. Sun, Curcumin inhibits proliferation and promotes apoptosis of breast cancer cells, Experimental and Therapeutic Medicine.

Spandidos Publications 16 (2018) 1266–1272, https://doi.org/10.3892/etm.2018.6345.
[73] M.A. Tomeh, R. Hadianamrei, X. Zhao, A review of curcumin and its derivatives as anticancer agents, Int. J. Mol. Sci. 20 (2019) 1033, https://doi.org/10.3390/ijms20051033.
[74] H. He, W. Zhuang, B. Ma, X. Su, T. Yu, J. Hu, et al., Oxidation-responsive and aggregation-induced emission polymeric micelles with two-photon excitation for cancer therapy and bioimaging, ACS Biomater Sci Eng. American Chemical Society 5 (2019) 2577–2586, https://doi.org/10.1021/acsbiomaterials.9b00212.
[75] K.-H. Jung, J.H. Lee, J.W. Park, D.H. Kim, S.-H. Moon, Y.S. Cho, et al., Targeted therapy of triple negative MDA-MB-468 breast cancer with curcumin delivered by epidermal growth factor-conjugated phospholipid nanoparticles, Oncol. Lett. 15 (2018) 9093–9100, https://doi.org/10.3892/ol.2018.8471.
[76] L. Bonilla-Vidal, M. Świtalska, M. Espina, J. Wietrzyk, M.L. García, E.B. Souto, et al., Dually active apigenin-loaded nanostructured lipid carriers for cancer treatment, Int. J. Nanomed. 18 (2023) 6979–6997, https://doi.org/10.2147/IJN.S429565. New Zealand.
[77] L. Santos Pimentel, S. Sommerfeld, P. Fernanda de Sousa Braga, A. Flores Coleto, B. Beatriz Fonseca, L. Machado Bastos, et al., Antitumor activity of essential oils-based nanostructured lipid carriers on prostate cancer cells, Int. J. Pharm. 657 (2024) 124149, https://doi.org/10.1016/j.ijpharm.2024.124149. Netherlands.